



Synergistic treatment of ovarian cancer by co-delivery of survivin shRNA and paclitaxel via supramolecular micellar assembly

Qinglian Hu^{a,1}, Wen Li^{a,1}, Xiurong Hu^a, Qida Hu^a, Jie Shen^a, Xue Jin^a, Jun Zhou^a, Guping Tang^{a,b,**}, Paul K. Chu^{b,*}

^a Institute of Chemical Biology and Pharmaceutical Chemistry, Zhejiang University, Hangzhou 310028, PR China

^b Department of Physics & Materials Science, City University of Hong Kong, Tat Chee Avenue, Kowloon, Hong Kong, PR China

ARTICLE INFO

Article history:

Received 20 March 2012

Accepted 27 May 2012

Available online 18 June 2012

Keywords:

Supramolecular micelles

Cancer treatment

siRNA

Paclitaxel

ABSTRACT

Non-viral gene-delivery platforms have been developed to co-deliver chemotherapeutics and siRNAs. The synergistic effects between shRNAs against survivin and Paclitaxel (PTX) using supramolecular micelles self-assembled from the host PEI-CyD (PC) composed of β -cyclodextrin (β -CyD) and polyethylenimine (PEI, Mw 600) and guest adamantine conjugated PTX (Ada-PTX) in combination cancer therapy are investigated. The Ada-PTX is encapsulated inside the core and shRNA sticks to the shell surface. The physicochemical properties of these supramolecular nanoparticles are favorable to cell uptake and intracellular trafficking. Moreover, PTX and shRNA simultaneously delivered to SKOV-3 cells lead to efficient reduction in the survivin and Bcl-2 expression as well as synergistic cell apoptotic induction in the *in vitro* study. In particular, co-delivery of survivin shRNA and PTX suppresses cancer growth more effectively than delivery of either paclitaxel or shRNA in ovarian cancer therapy.

© 2012 Elsevier Ltd. All rights reserved.

1. Introduction

Chemotherapy is the treatment of choice for many types of cancers, but its success is often hampered by development of drug resistance after repeated administration. RNA interference (RNAi), a promising approach in cancer therapy, can selectively down-regulate target gene expression, overcome the multi-drug resistance, and improve the sensitivity of chemotherapeutic drugs [1–3]. RNAi is often mediated by short hairpin RNAs (shRNA) or small interfering RNAs (siRNA). ShRNA is a sequence of RNA which makes a tight hairpin turn and cloned into expression vectors to ensure that the shRNA is always expressed. Moreover, by including inducible elements in the promoter, the expression of shRNA is inducible. Survivin, the inhibitor of the apoptosis protein family as a new target in anti-cancer therapy, is involved in cancer progression and treatment of resistance [4,5]. RNAi targeted survivin has

been reported to increase the human tumor sensitization to chemical and physical agents [6,7].

PTX derived from the bark of the pacific yew tree has the unique ability of promoting the microtubular assembly and stability, thereby inhibiting mitotic progression and inducing cellular apoptosis [8,9]. PTX provides treatment benefits for broad range of solid tumors, especially in breast and ovarian cancer, but the therapeutic effectiveness is heretofore limited due to the poor aqueous solubility of the drug, acquired chemo-resistance of cells, and side effects [10]. Hence, formulation of PTX based on nanotechnology, including polymeric micelles, nanoparticles, and liposomes, can increase the paclitaxel solubility [11–13] and address drug resistance [14,15]. In this respect, a nanocarrier-based delivery system offers a platform for the co-delivery of siRNA and anti-cancer chemotherapeutics. For example, multifunctional liposomes can co-deliver siRNA and doxorubicin to overcome the drug resistance [16] and mesoporous silica nanoparticles have been reported to co-encapsulate siRNA targeted Bcl-2 with doxorubicin to enhance the efficiency of chemotherapy in multi-drug cancer cells [17]. Moreover, polymeric micelles have been adopted as carriers in the simultaneous delivery of siRNA and anti-cancer drugs [14,18–20].

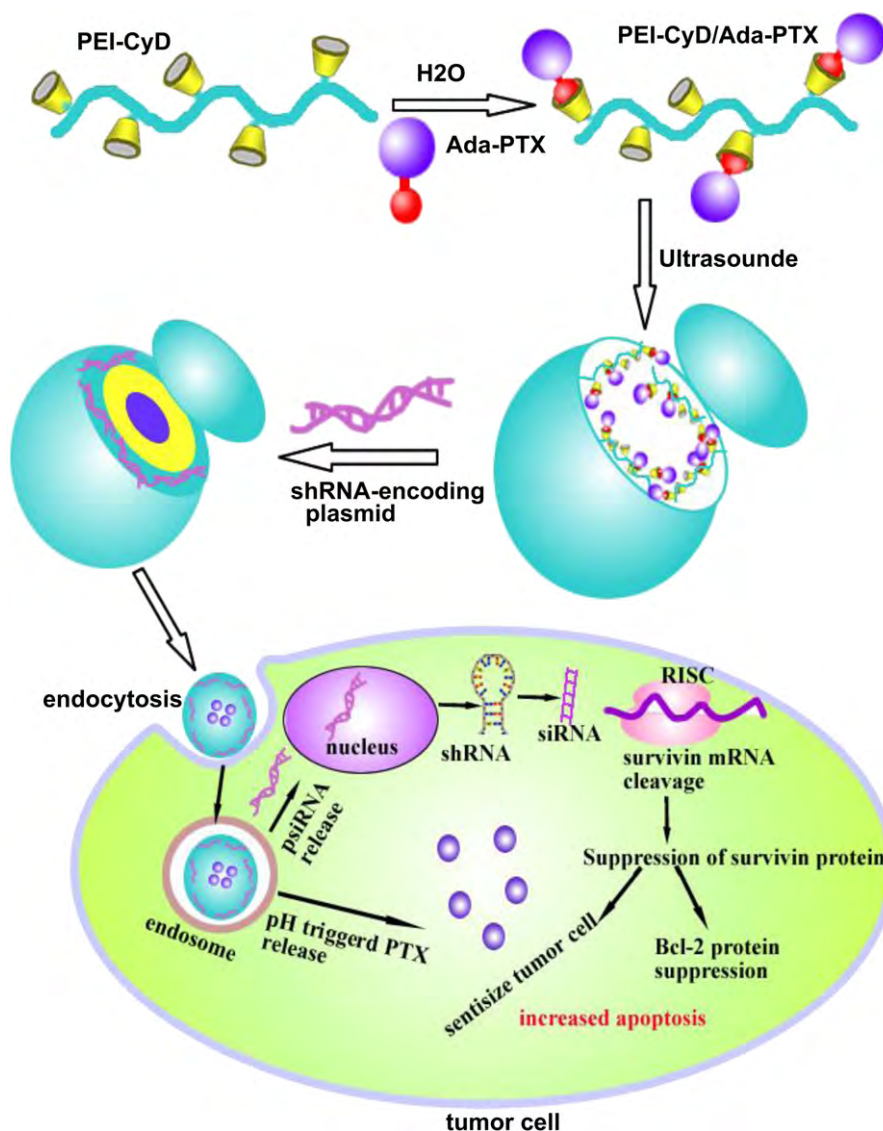
We have recently reported the use of supramolecular nanoparticles and subsequent host-guest interactions to achieve simultaneous delivery of doxorubicin and therapeutic gene TRAIL

* Corresponding author. Tel.: +86 852 34427724; fax: +86 852 34420542.

** Corresponding author. Institute of Chemical Biology and Pharmaceutical Chemistry, Zhejiang University, Hangzhou 310028, PR China. Tel./fax: +86 571 88273284.

E-mail addresses: tangguping@zju.edu.cn (G. Tang), paul.chu@cityu.edu.hk (P.K. Chu).

¹ Both authors contributed equally to this work.



Scheme 1. Schematic illustration of co-delivery of shRNA and PTX using supramolecular nanoparticles.

in cancer treatment [21,22]. In the work described in this paper, we fabricated cationic micelles self-assembled from supramolecular nanoparticles (SNPs) produced by β -cyclodextrin-polyethyleneimine (PEI-CyD) and 2-amineadamantane-conjugated paclitaxel (Ada-PTX) to deliver PTX and survivin shRNA-encoding plasmids to SKOV-3 cells simultaneously. Ada-PTX as a core was physically encapsulated into the micelles and survivin shRNA adsorbed on the shell of the cationic micelles. The physicochemical properties such as morphology, size, and zeta potential as well as release properties were determined and the ability and synergistic therapeutic effects of co-delivering PTX and shRNA to tumor cells were demonstrated *in vitro* and *in vivo*.

2. Materials and methods

2.1. Materials

Polyethyleneimine (branched PEI, MW 600 Da and 25 KD), β -cyclodextrin (β -CyD, MW 1135), 1,1'-carbonyldiimidazole (CDI, MW 162.15), 4-dimethylaminopyridine (MW 122.17), succinic anhydride (MW 100.07), adamantylamine (MW 151.25), [3-(4,5-dimethylthiazol-2-yl)-2,5-diphenyltetrazolium bromide] (MTT, MW 218.1), and triethylamine (Et_3N , $\geq 99\%$) were obtained from Sigma (St. Louis, MO, USA). Paclitaxel (PTX, MW 853.91, 99.5%) and rhodamine labeled paclitaxel were

purchased from Hao-Xuan Biotechnology Co., Ltd. (Xi'an, China). Fluorescein-tagged siRNA (FAM-siRNA), survivin shRNA-encoded plasmid (sequence: ACCGCATCTCTCAATTCAAGA) and scramble shRNA-encoding plasmid (SR) were obtained from Genechem Co., Ltd. (Shanghai, China).

The human ovarian cancer cell line SKOV3 was purchased from American Type Culture Collection (Rockville, MD) and cultured in RPMI 1640 culture medium supplemented with 10% fetal bovine serum (FBS). The cells were cultured at 37 °C in a humidified atmosphere containing 5% CO_2 . Athymic female mice (BALB/c strain) (4–6 weeks old and 18–22 g in weight) were purchased from the Zhejiang University Animal Care Center and maintained in a pathogen-free environment at a controlled temperature of 24 °C. The animal experiments were performed in accordance with the CAPN (China Animal Protection Law) and the protocols were approved by the Zhejiang University Animal Care and Use Committee.

2.2. Synthesis and Biochemical Characterization of PC/Ada-PTX

The PC was prepared as described previously [24]. Paclitaxel (1, 170.6 mg, 0.2 mmol) was added to succinic anhydride (70 mg, 0.7 mmol) in the presence of 4-dimethylamino-pyridine (41 mg, 0.33 mmol). Five ml of dry pyridine was added and the solution was stirred for 3 h at room temperature. The 2'-succinyl-paclitaxel was purified by extraction according to following procedures. After 20 mL of dry dichloromethane (DCM) had been added to the mixture, the organic phase was washed using 1 M HCl (20 mL \times 3) and water (20 mL \times 3) and the water phase was extracted by DCM (10 mL \times 3). The organic phase was combined and washed by brine (10 mL \times 3) and dried over Na_2SO_4 . The filtrate was concentrated on a rotary

Table 1
Physicochemical properties of synthesized PC and PC/Ada-PTX.

Type of products	PEI CyD: PTX (W/W)	Drug content (w/w, %)	CMC (mg/ml)	Particle size (nm)	Zeta potential (mv)
PC/ShRNA	—	—	—	185 ± 5	21.2 ± 1.3
PC/Ada-PTX-1	5:1	0.28 ± 0.05	0.032	194 ± 7	20.5 ± 2.3
PC/Ada-PTX-2	3:1	1.07 ± 0.16	0.025	207 ± 9	19.5 ± 3.5
PC/Ada-PTX3	2:1	3.42 ± 0.71	0.016	220 ± 5	18.2 ± 1.9
PC/Ada-PTX4	1:1	6.13 ± 1.07	0.013	228 ± 4	17.3 ± 4.1
PC/Ada-PTX-3 /ShRNA	2:1	3.42 ± 0.71	0.016	210 ± 8	16.2 ± 5.7

CMC: Critical micelle concentration in DI water solution.

Drug content: the weight ratio of PTX and PC in the final product PAP.

Particle size and Zeta potential: Data representing the mean ± standard deviation ($n = 3$).

In the study, PC/Ada-PTX-3 is used.

evaporator and the crude product was used without further purification. 2'-succinyl-paclitaxel (48.3 mg, 0.05 mmol) and CDI (15.1 mg, 0.093 mmol) were dissolved in DMSO (1 mL), respectively and the CDI solution was added slowly to the 2'-succinyl-paclitaxel solution dropwise at room temperature under nitrogen. After mixing with Et₃N (200 μL), it was stirred for 3 h. Ada-NH₂ (10.0 mg, 0.066 mmol) was dissolved in DMSO (2 mL) and added dropwise to the 2'-succinyl-paclitaxel solution. The mixture was stirred overnight under nitrogen to yield Ada-PTX. Afterward, distilled water (10 mL) was added and it was stirred for 30 min to remove excess CDI. Different amounts of PC (51.1 mg, 106.8 mg, 150.2 mg, 261.0 mg) were dissolved in H₂O (15 mL) and added dropwise to Ada-PTX. The resulting

mixture was stirred for 8 h followed by dialysis in water for 24 h, then filtered to remove the precipitation and freeze-dried to yield purple PC/Ada-PTX (PAP) powders.

The critical micelle concentration (CMC) of PAPs was determined by fluorescence measurement using pyrene as the probe. The excitation wavelength was 337 nm, excitation slit was 2.5 nm, and emission slit was 10 nm. The emission between 360 and 450 nm was monitored by a fluorescence spectrophotometer. The concentration of PAPs was between 5.0×10^{-4} to 1.0 mg/ml and that of pyrene was 6×10^{-7} mol/L. The intensity ratio of the first peak (I_1 , 374 nm) to the third peak (I_3 , 385 nm) was calculated from results obtained on the CMC (F-25000, Hitachi Co., Japan).

The ¹H and 2D-NOESY NMR spectra of each sample were acquired on a Bruker DRX-400 spectrometer (Bruker, Ettlingen, Germany) at room temperature using DMSO-*O*₆ as the solvent. The chemical structure of the polymers was also evaluated by Fourier-transform infrared spectroscopy (FT-IR, Varian, Excalibur™, USA).

The particle size and zeta potential were determined at 25 °C by dynamic light scattering (DLS) on the Zetasizer 3000 (Malvern Instruments, Worcestershire, UK). The morphology of the complexes was examined by field-emission scanning electron microscopy (FE-SEM, JEOL JSM-7400F, Japan) and transmission electron microscopy (Tecnai 10, TEM). Gel electrophoresis was performed at room temperature in the TAE buffer in 1% (w/w) agarose gel at 80 V for 40 min and the DNA was visualized by a UV (254 nm) illuminator.

2.3. *In vitro* release of PTX

The *in vitro* release of PTX from PAP was monitored using the dialysis method. The PAP and PAP/shRNA complexes were dissolved in phosphate buffer solutions at pH values of 5.0 and 7.4, sealed in dialysis bags with a molecular weight cut-off of 8 kDa to 14 kDa. The apparatus was agitated on an orbital shaker at 100 rpm at 37 °C. At designated time intervals, the medium was removed and replaced by a fresh one. The amount of PTX released into the medium was determined from the absorbance

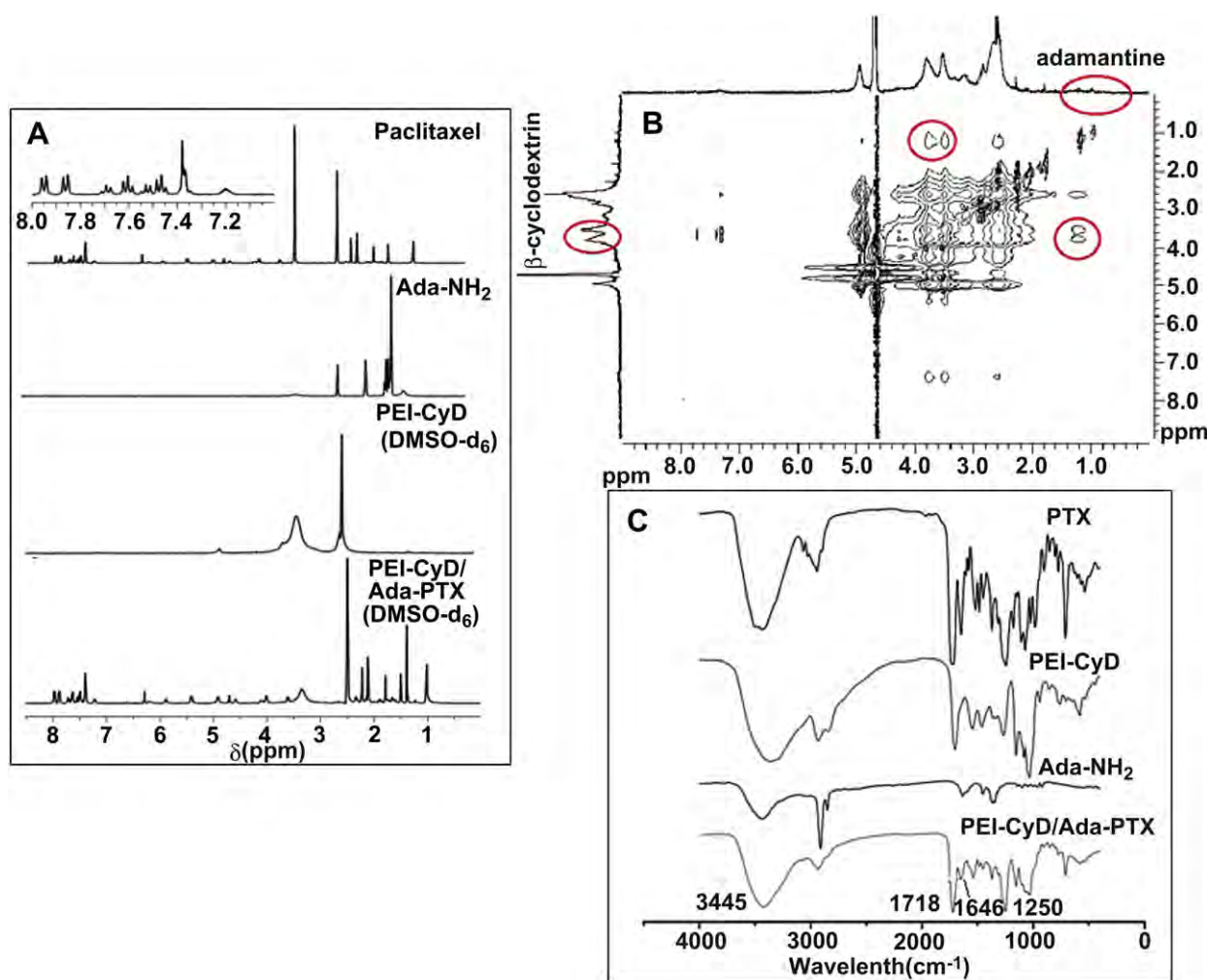


Fig. 1. (A) ¹H NMR spectra of PTX, Ada-NH₂, PC and PAP in DMSO-*d*₆; (B) 2D-NOESY NMR spectrum of PAP in D₂O; (C) FTIR spectra of PTX, Ada-NH₂, PC and PAP.

at 227 nm by high-performance liquid chromatography (HPLC) (1100 HPLC, Agilent Technologies, Santa Clara, CA).

2.4. Cellular uptake Investigation

The cell uptake and distribution were examined by confocal microscopy. 5×10^4 well SKOV-3 cells were seeded onto 24-well plates and grown for 18 h. The PAP containing Rhodamine-labeled paclitaxel was synthesized as described before. 0.5 μg of FAM-siRNA was complexed with PAP^(Rho-PTX) at N/P 25 at room temperature for 20 min before use. After transfection for 2 h, the cells were fixed with fresh 4% paraformaldehyde and treated with 10 $\mu\text{g}/\text{ml}$ hoechst33245 in PBS for 10 min. The confocal images were acquired on a confocal scanning laser microscope (CLSM, Radiance 2100, Bio-Rad).

2.5. In vitro transfection

The survivin shRNA and negative control shRNA which had the EGFP reporter fuse gene were utilized to determine the efficiency of the polymer. 1 μg of the survivin shRNA or control shRNA was complexed with PC or PAP at N/P 25 at room temperature for 20 min. The transfection experiments with Lipofectin2000 were performed according to the manufacturer's instructions. The cells were cultured and transfected. After incubation for 36 h, the cells were observed by fluorescence microscopy. The fluorescence photographs of the GFP positive SKOV-3 cells were taken by a Leica (DMLB&DMIL) microscope equipped with a Digital 1/2 inch CCD and Leica MPS 60.

2.6. In vitro analysis of survivin and Bcl-2 expression

The SKOV-3 cells were seeded in 6-well culture plates at a density of 2.5×10^5 cells per well in 2 mL of the complete RPMI 1640 culture media and incubated at 37 °C in 5% CO₂ for 18 h to reach 70% confluence. The dose of shRNA per 6-well was 4 μg and the equivalent dose PTX was 1.2 μg . The moderate and high doses of PTX were 6 μg and 24 μg , respectively. The cellular levels of survivin and Bcl-2 mRNA and protein were assessed using quantitative real-time PCR (qRT-PCR) and Western blot at 24 h and 48 h, respectively.

In the RT-PCR analysis, mRNA was extracted from a total of 1×10^6 cells after 24 h and 48 h of transfection and then reverse-transcribed into cDNA by using Qiagen RNEasy Mini Kit (Cat. No.74104). Quantification of the PCR product was performed in

1 \times TE buffer using absorption values at 260 nm and 280 nm ($c(\text{RNA}) = \text{OD}_{260} \times \text{dilution factor} \times 0.04 \mu\text{g}/\mu\text{L}$). The RNA was reverse-transcribed with OligodT (Fermentas) according to the protocol. The relative gene expression values were determined using the BandScan4.3 software and the data presenting the survivin and Bcl-2 expression were normalized to the housekeeping gene β -actin as the endogenous reference. The primers used in RT-PCR for survivin, Bcl-2, and β -actin were: survivin-forwards 5'- GTCTGGCGTA AGATGATGGA -3', survivin-reverse 5'- GGAGCCCGGATGATAC AA-3', Bcl-2-forward 5'- GTGGAGGAGCTCTCAGGGA -3', Bcl-2 reverse 5'- AGGCCACCCAGGGTGATGCAA -3', and actin forward 5'- GCTCGTCGTCGACAC A GGCTC -3', and actin reverse 5'- CAAACATGATCTGG GTCATCTTCTC -3'. The PCR parameters consisted of 5 min of Taq activation at 95 °C, followed by 28 cycles of 95 °C \times 40 s, 56 °C \times 30 s, and 72 °C \times 35 s.

In the Western blotting analysis, the cells were transfected as described above and the cell proteins were extracted after transfection for 24 h and 48 h. The total protein was quantified by the BCA protein assay kit (Promega, USA). An equal amount of protein was separated on the SDS-PAGE, transferred onto nitro-cellulose membrane, and blocked and incubated overnight with monoclonal antibodies against survivin (1:400) and Bcl-2 (1:400) overnight. After washing, the membrane was incubated with HRP-conjugated secondary antibody (1:5000) for 2 h at room temperature. The bands were visualized using the Westzol enhanced chemiluminescence kit (Intron, Sunngam, Korea) and the expression was normalized with housekeeping gene expression.

2.7. Cell apoptosis analysis

In the apoptosis analysis, the SKOV-3 cells cultured in 6-well plates were treated with the mentioned formulations. After treatment for 48 h, the rate of apoptosis was measured by the Annexin V-FITC Apoptosis Detection Kit (KeyGEN, Jiangsu, China) in accordance with the manufacturer's protocol. In brief, the cells were detached with the EDTA-free trypsin solution, collected, washed twice with phosphate-buffered solution (PBS), and resuspended in 500 μL of annexin V binding buffer at a concentration of 5×10^5 cells/mL. 5 μL of FITC-conjugated annexin V and 5 μL of propidium iodide (PI) were added to the cells and incubated for 15 min at room temperature in the dark before the flow cytometric analysis. A minimum of 10,000 cells were analyzed in each sample using an EPICS XL flow cytometer (Beckman-Coulter, USA). The fluorescence measurements were conducted at an excitation wavelength of 488 nm (Ex) and emission wavelength of 530 nm (Em) and the untransfected cells were used to obtain the background.

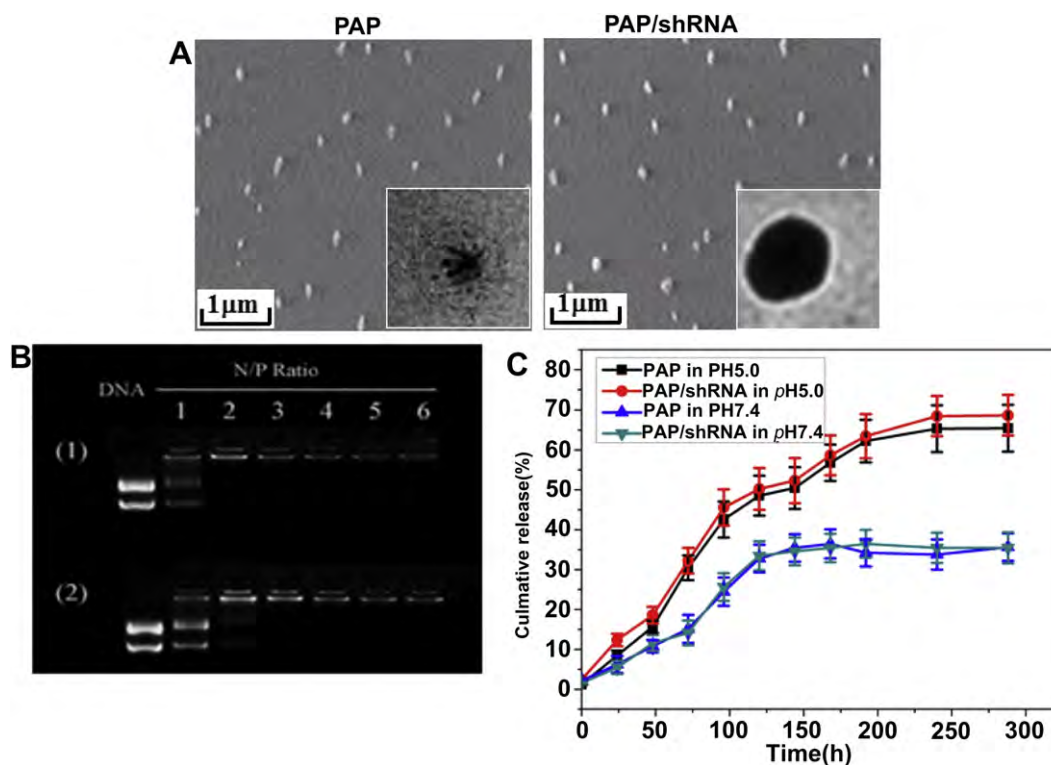


Fig. 2. (A) SEM and TEM (inset) images of PAP and PAP/shRNA; (B) Electrophoretic mobility of pDNA in the complexes of PC (upper panel) and PAP (lower panel); (C) Drug release from PAP and PAP/shRNA at pH 7.4 and pH 5.0.

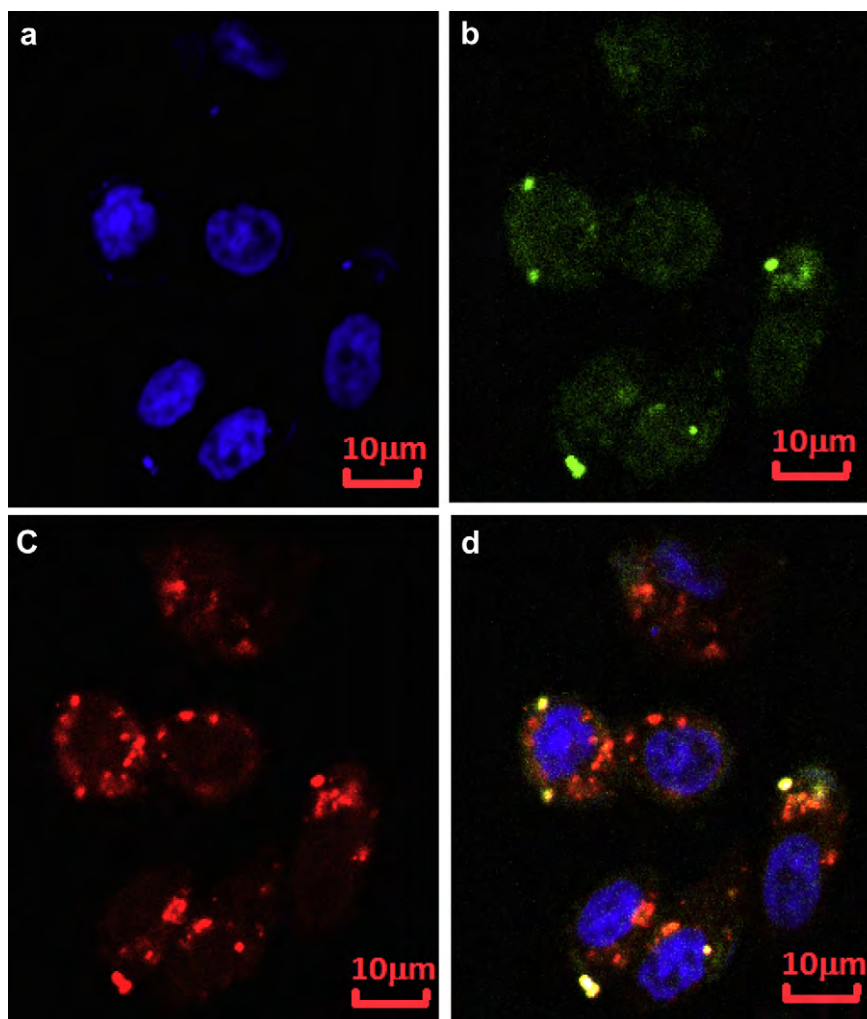


Fig. 3. Confocal images of the cellular uptake induced by PAP/shRNA in SKOV-3 cells: (a) Nucleus stained blue; (b) Green fluorescence (FAM-siRNA), (c) Red fluorescence (PTX-rhodamine) images and (d) Merged image.

2.8. Cell viability assay

The cytotoxicity of the complexes was evaluated using the MTT assay. The SKOV-3 cells were seeded in 96-well plates at a density of 8000 cells/well for 24 h. The cultural medium was then replaced by a serum-free medium containing various concentrations of free PTX, PAP, PC/shRNA, PC/shRNA + PTX, PAP/shRNA and PAP/SR. After 24 h, the medium was replaced with a fresh growth medium and after 48 h or 72 h, the culture medium was replaced by the MTT solution for 4 h. After removal of MTT medium, the formazan crystals were dissolved in DMSO and the microplates were agitated for 10 s at a medium rate prior to the spectrophotometrical measurement at the wavelength of 570 nm on an ELISA reader (Model 680, Bio-Rad). The untreated cells served as the 100% cell viability control and the completely died cells served as the blank. The relative cell viability (%) related to control cells was calculated by the formula below:

$$V\% = \frac{[A]_{\text{experimental}} - [A]_{\text{blank}}}{[A]_{\text{control}} - [A]_{\text{blank}}} \times 100\%$$

where V% is the cell viability (%), $[A]_{\text{experimental}}$ is the absorbance of the wells culturing the treated cells, $[A]_{\text{blank}}$ is the absorbance of the blank, and $[A]_{\text{control}}$ is the absorbance of the wells culturing untreated cells. The 50% inhibitory concentration (IC_{50}) was determined by fitting the data to the following equation:

$$V\% = \frac{100}{1 + ([PTX]/IC_{50})^p}$$

where V% is the viability (%), [PTX] is the concentration ($\mu\text{g mL}^{-1}$) of the paclitaxel or equivalent paclitaxel in PAP in a well, and p was defined as the slope of the sigmoid curve.

2.9. In vivo tumor growth and Survival rate Assessment

BALB/c nude mice bearing SKOV-3 ovarian tumors were randomly assigned to five groups when the tumors volume reached around 50 mm^3 12 days after tumor inoculation. Each group consisted of five mice. The doses of shRNA of each injection were fixed at $20 \mu\text{g}$ and the equivalent dose of PTX was $6 \mu\text{g}$. The treatment was performed twice a week for 2 weeks and the tumor growth was monitored using calipers twice a week. The tumor volume (V) was calculated by the following formula: tumor volume $V(\text{mm}^3) = \pi/6 \times \text{length}(\text{mm}) \times \text{width}(\text{mm})^2$. Three mice from each group were sacrificed 30 Days later after first injection. Their tumors were dissected, weighed, and then imaged. The other tumor-bearing mice were continuously observed for up to three months and differences in tumor growth were tested for statistical significance.

2.10. Statistical analysis

All the experiments were repeated at least three times and the data were presented as means \pm standard deviation. The statistical significance ($p < 0.05$) was evaluated by the student t -test when only two groups were compared. If more than two groups were compared, evaluation of significance was performed using one-way analysis of variance (ANOVA) followed by Bonferroni's post hoc test. In all the tests, the statistical significance was set at $p < 0.05$.

3. Results and discussion

3.1. Synthesis and characterization of supramolecular micelles

β -CyD and Ada are widely employed in macromolecular assembly due to the strong binding ability with an association

constant around 1×10^5 mol/L in water [23]. Our results demonstrate that supramolecular polymers can form core-shell nanoparticles with a hydrophobic core (Ada-PTX) and cationic shell (PC) in an aqueous solution by a self-assembly process (Scheme 1). In the supramolecular micelles, PTX is conjugated to the core and shRNA adsorbs on the shell surface. It is hypothesized that survivin shRNAs delivered to the cells will down-regulate the target genes and sensitize the tumor cells to the co-delivered PTX, resulting in an enhanced therapeutic activity of the nanomedicine.

The cationic supramolecular polymers are produced derived by a three-step synthesis illustrated in Scheme 2. The PC copolymers are first synthesized from PEI ($M_w = 600$ Da) and β -CyD [24], the PTX is modified by 2-amineadamantyl (Ada-NH₂) via amide linkage to form Ada-PTX, and then the Ada-PTX molecules form complexes with the PC copolymer in PBS by host-guest interactions resulting in the supramolecular polymers PC/Ada-PTX (PAP). The PAPs are synthesized by changing the amount of PTX (Table 1). The chemical structure of the supramolecular conjugates are characterized by ¹H NMR (Fig. 1A), 2D Nuclear Overhauser Spectroscopy (NOESY) spectrometry (Fig. 1B), and FTIR (Fig. 2C). The ¹H NMR spectra of PTX, Ada-NH₂, PC, and PC/Ada-PTX are shown in Fig. 1A. The protons at δ 1.0–2.0 ppm and δ 7.0–8.0 ppm are assigned to the methyl and phenyl groups of PTX whereas those at δ 1.5–2.0 ppm correspond to adamantyl of Ada-NH₂. The protons at δ 2.3–2.8 ppm are assigned to PEI (–CH₂–CH₂–NH–) and those at δ 3.0–4.0 ppm are associated with the methoxyl groups of PC. The small peaks related to PTX, Ada-NH₂, and PC can be observed from the spectrum of PAP. In 2D nuclear Overhauser spectroscopy (NOESY), all three signals of the methylene and methine protons of adamantyl moiety are well correlated with the inner protons of β -CyD (Fig. 1B). The FTIR results provide additional chemical structure

information and the strong carbonyl bands at 1718 cm⁻¹ and 1646 cm⁻¹ in Fig. 1C confirm the presence of ester carbonyl and acylamino from Ada-PTX. The broad stretching vibration at \sim 3445 cm⁻¹ suggests the existence of hydroxyl and amino groups in the PC/Ada-PTX and all of them indicate the formation of supramolecular inclusion complexes.

The PAPs can self-assemble to form micelles in an aqueous medium. The critical micelle concentration (CMC) is an important parameter of amphiphilic materials indicating the micelle formation ability. The aggregation behavior of PAPs is measured by fluorometry using a pyrene probe. Table 1 reveals that the CMC value is reduced with increasing grafting ratio of PTX. The PAPs can self-assemble to form micelles enabling fast internalization into tumor cells due to the spatial structure with a multi-hydrophobic core. The relatively low CMC value (close to 0.02 mg/ml) is attributed to paclitaxel, because as the amount of PTX in the host-guest polymer is increased, the hydrophilic and hydrophobic blocks come to a balance and the polymer can disperse easily in the medium forming micelles.

To evaluate the feasibility of using the polymers to co-deliver drug and shRNA, the physicochemical properties such as morphology, particle size, and zeta potential, as well as release properties are investigated. The polymer forms a micellar structure in the aqueous solution, with PTX conjugated to the core and shRNA on the shell surface. As shown in Table 1, the PAP has an average size of 220 nm and zeta potential of 18.2 mV. Formation of the supramolecular micelles results in a size increase compared to PC (185 nm) and zeta potential reduction (21.2 mV). The PAP complexed with shRNA exhibits slight changes in size (210 nm) and zeta potential (16.2 mV). The supramolecular micelles possess a compact and spherical morphology as revealed by scanning

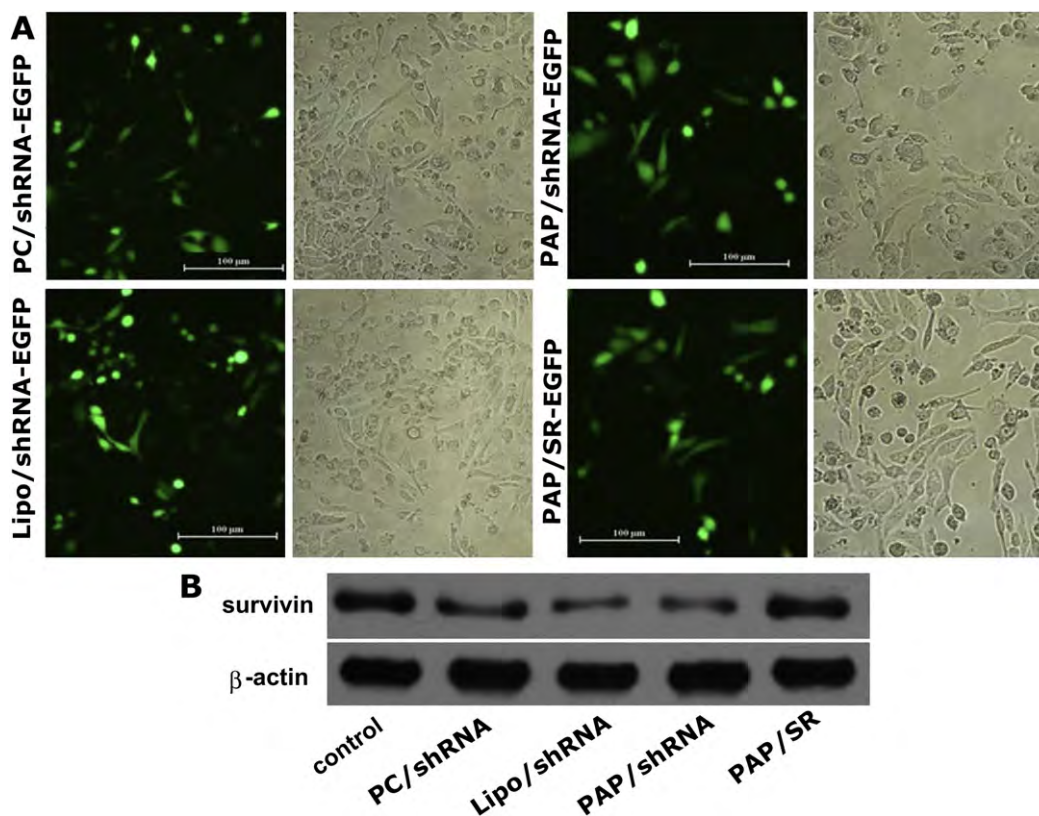


Fig. 4. Fluorescence (left panel) and differential interference contrast (DIC) (right panel) images (A) and Western blot analyses of survivin (B) with survivin shRNA and scrambled shRNA transfected by PC, PAP and Lipofectin2000 in SKOV-3 cells.

electron microscopy (SEM) and transmission electron microscopy (TEM) and the results are consistent with those in Table 1 (Fig. 2A). ShRNA complexed with PAP has decreased mobility in the electromobility shift assay (Fig. 2B) and complete retardation of the shRNA is achieved at an N/P ratio (molar ratio of nitrogen content in the polymer to phosphorous content in the DNA) of 2 and 3 for PC and PAP, respectively. The DNA-binding ability of the PC is slightly greater than that of the PAP due to perhaps inclusion of the guest shielding primary amines of the PC.

The PTX release behavior from the PAP and PAP/shRNA is studied and compared in aqueous solutions at pH of 7.4 and 5.0 at 37 °C. As shown in Fig. 2C, the PAP and PAP/shRNA show the same

release behavior. The drug is gradually released even after 150 h, indicating that PAP prolongs the circulation time of paclitaxel, reduces its degradation in the body fluid, decreases drug-related side effects, and increases drug efficacy. Comparing the drug release profiles at the two pH values, release of PTX from the micelles at the low pH is swifter. This pH-dependent release enables preferential release of PTX from the endosome of tumor cells due to the acidic environment. Hence, it is expected that after the PAP/shRNA enter the cancer cells, PTX will be released at the endosomal acidic pH and shRNA escapes simultaneously from the endosome due to the proton sponge effect of PEI [25] and then translocates to the nucleus.

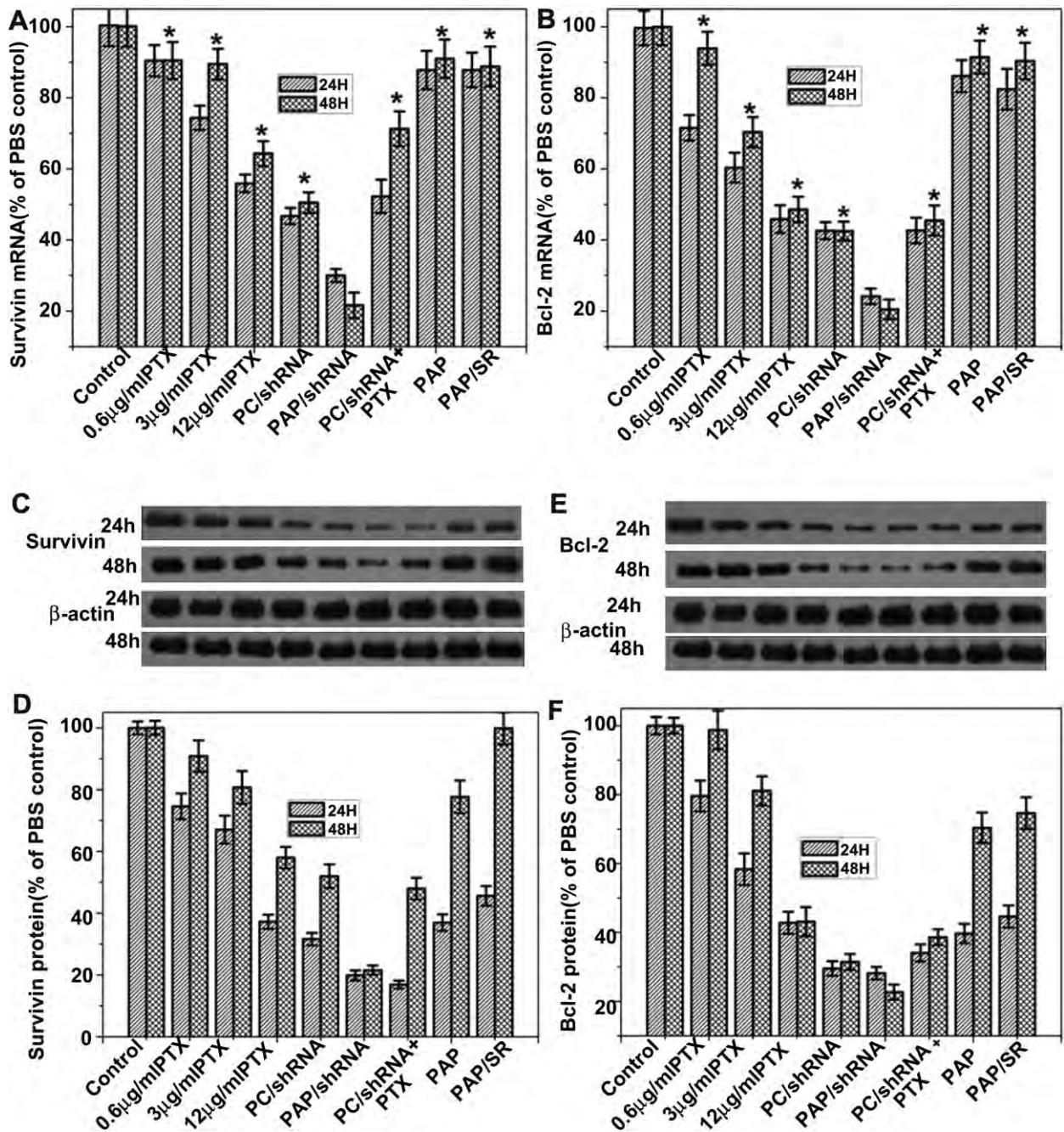


Fig. 5. Expression of survivin and Bcl-2 mRNA determined by quantitative real-time PCR at 24 h and 48 h (A and B); representative survivin and Bcl-2 protein expression determined by Western blot analysis (C and E); analysis of light intensities of survivin and Bcl-2 protein expression from Western blot results (D and F).

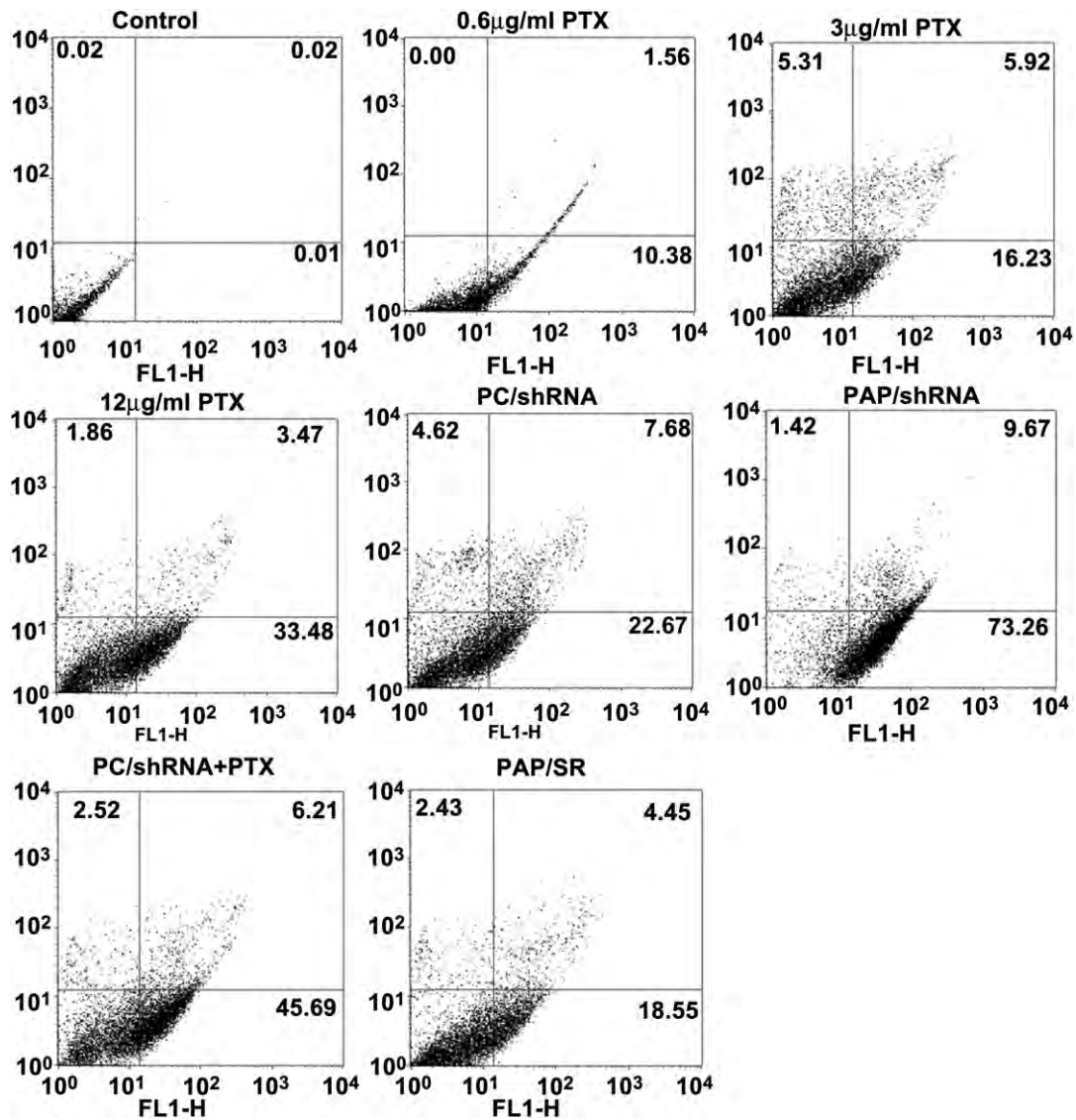


Fig. 6. Induction of apoptosis on SKOV-3 cells by PAP and other formulations.

3.2. Cellular uptake and transfection of shRNA

To demonstrate simultaneous delivery, we first analyze the cellular uptake and intracellular distribution of PAP/FAM-siRNA in SKOV3 cells by confocal microscopy with the paclitaxel labeled with rhodamine. Colocalization of the PTX and siRNA in the same cells is observed by confocal laser scanning microscopy (Fig. 3 - internalized PTX-rhodamine: red; FAM-siRNA: green; nuclei: blue). The observation indicates that the PAP is able to simultaneously deliver the drug and siRNA to cells giving rise to cooperative effects on the cancer cells.

RNAi is often mediated by short hairpin RNAs (shRNA) or small interfering RNAs (siRNA). Here, survivin shRNA-encoding plasmid with reporter EGFP fusion gene is chosen to silence the expression of the survivin gene. Although direct delivery of synthetic siRNA may be more effective for non-dividing cells, the gene-silencing effect is transient and non-inducible [26]. The shRNA-encoding plasmid requiring intra-nuclear localization can express siRNA in a stable and inducible manner in fast dividing mammalian cells. Therefore, for rapidly growing cancer cells, the shRNA-encoding plasmid system ought to be more efficient. The EGFP gene

transfection in this system is illustrated in Fig. 4A showing that PAP can transfect SKOV-3 similar to PC and lipofectin2000. The results also suggest that the PTX-loaded supramolecular micelles can achieve high gene transfection and that the shRNA-encoding plasmid against survivin and scramble shRNA-encoding plasmid can effectively enter the nucleus and express. Suppression of the survivin expression by shRNA is assessed by Western-Blot (Fig. 4B). The PC, PAP, and lipofectin2000 complexed with survivin shRNA

Table 2
Summary of cell apoptosis analysis by flow cytometry.

Materials	Apoptotic cells(%)	Normal cells(%)
Control	0.03	99.95
PTX(0.6 μg/ml)	11.94	88.06
PTX(3 μg/ml)	22.15	72.54
PTX(12 μg/ml)	36.95	61.19
PC/shRNA	30.35	65.03
PAP/shRNA	82.93	15.65
PC/shRNA + PTX	51.90	45.58
PAP/SR	22.00	74.57

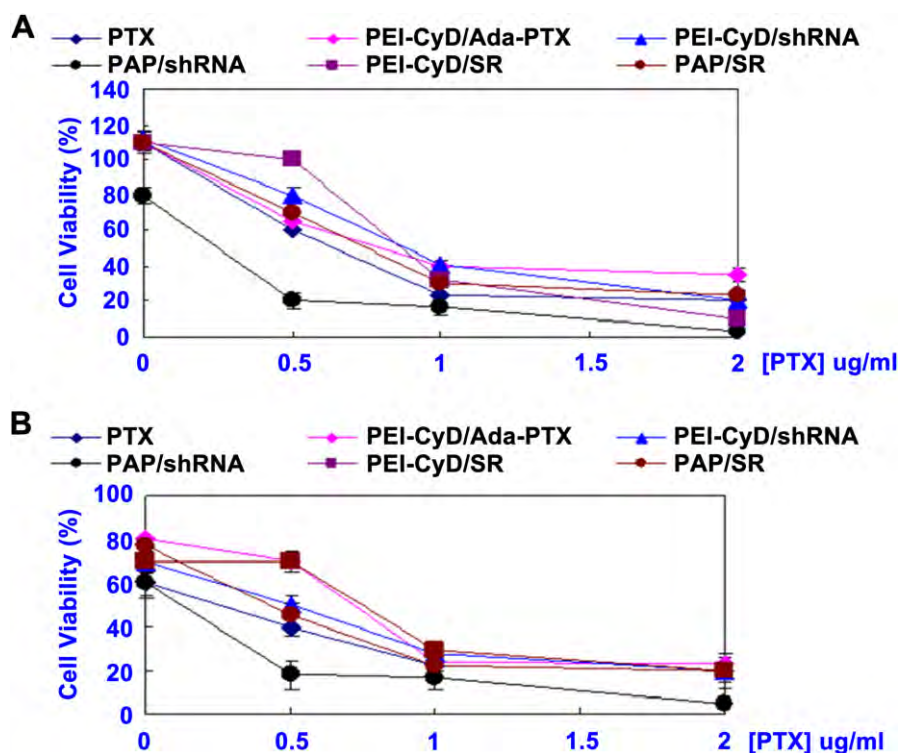


Fig. 7. Cell viability of PTX, PAP, PC/shRNA, PAP/shRNA, PC/SR and PAP/SR in SKOV-3 cells at 48 h (A) and 72 h (B).

show obvious decrease in the survivin expression and the scrambled shRNA has no effect on the gene expression of survivin. The results suggest that the shRNA-encoding plasmid against the survivin systems can induce efficient gene-knockdown of the target gene and the PAP-based shRNA delivery system is excellent.

3.3. Synergistic effects of survivin shRNA and PTX in vitro

To gain further insight into the synergistic effects of the supramolecular nanocarriers co-delivering PTX and shRNA, the mRNA and protein level of survivin and Bcl-2 are assessed 24 h and 48 h after transfection. Bcl-2 is the most important anti-apoptotic protein, which is predominantly found in the outer mitochondrial membrane, acts effectively through the mitochondrial-dependent cell apoptosis pathway [27]. The apoptotic response of SKOV-3 cells after the treatment is assessed by detecting Bcl-2 as an indicator of the apoptosis pathway. We evaluate the effects of concentration of free PTX and different formations on the suppression of survivin and Bcl-2 expression. The three PTX concentrations of 0.6 µg/ml, 3 µg/ml, and 12 µg/ml, represent low (equal to the PAP dose), moderate, and high dose respectively. As shown in Fig. 5A, a low dose of free PTX treatment as well as PAP and PAP complexed with scrambled shRNA only have a small effect on the mRNA level of the survivin. The survivin mRNA expression is reduced in a PTX dose and time dependent manner. A large free PTX concentration produces better gene-silencing efficacy and as the incubation time is increased, the survivin mRNA is up-regulated. For example, 12 µg/ml of PTX leads to ~45% and ~36% knockdown of survivin mRNA at 24 h and 48 h, respectively. Compared to PC/shRNA (~54%, ~50%) and PC/shRNA + PTX (48%, 29%), co-delivery of shRNA and PTX shows the most obvious inhibition in the survivin mRNA expression (70% and 79%) at 24 h and 48 h. It is worth noting that except for PAP/shRNA, other treatments achieve the higher efficiency of survivin knockdown at 24 h. As the

incubation time is increased, the survivin mRNA up-regulates indicating that simultaneous delivery of the drug and shRNA to the same cell by PAP not only exerts cooperative effects but also prolongs the effective time. The Bcl-2 mRNA exhibits the same trends as survivin (Fig. 5B). The decreased survivin and Bcl-2 protein expression is also verified by the Western blot analyses (Fig. 5C, D, E and F). The PAP/shRNA results in most efficient survivin and Bcl-2 down regulation at time points of 24 h or 48 h.

Survivin is associated with microtubules and with the mitotic spindle, results in cell division and apoptosis suppression [28,29]. Knockdown of survivin has been shown to induce apoptosis in tumor cells [2,6,30]. Apoptosis is the primary mode of cell death induced by several classes of anti-cancer agents. It is postulated that suppression of survivin in combination with cell death induced by PTX can influence the apoptotic response of SKOV-3. Apoptosis is evaluated by Annexin-V-FITC and propidium iodide (PI) staining. The flow cytometry data about cell apoptosis from different groups are shown in Fig. 6 and Table 2. Not surprisingly, co-delivery of PTX and survivin shRNA leads to the highest rate of cell apoptosis 82.93%, which is clearly superior to that of PC/shRNA (~30.35%) and a simple mixture of gene and drug (PC/shRNA + PTX, 51.9%). The

Table 3
Values of IC₅₀ treated with various formulations.

Compounds	IC ₅₀ [equivalent to PTX] (µg mL ⁻¹)	
	48 h	72 h
PTX	0.591	0.296
PEI-CyD/Ada-PTX	0.700	0.469
PEI-CyD/shRNA	0.774	0.530
PEI-CyD/Ada-PTX/shRNA	0.194	0.099
PEI-CyD/SR	0.925	0.704
PEI-CyD/Ada-PTX/SR	0.669	0.372

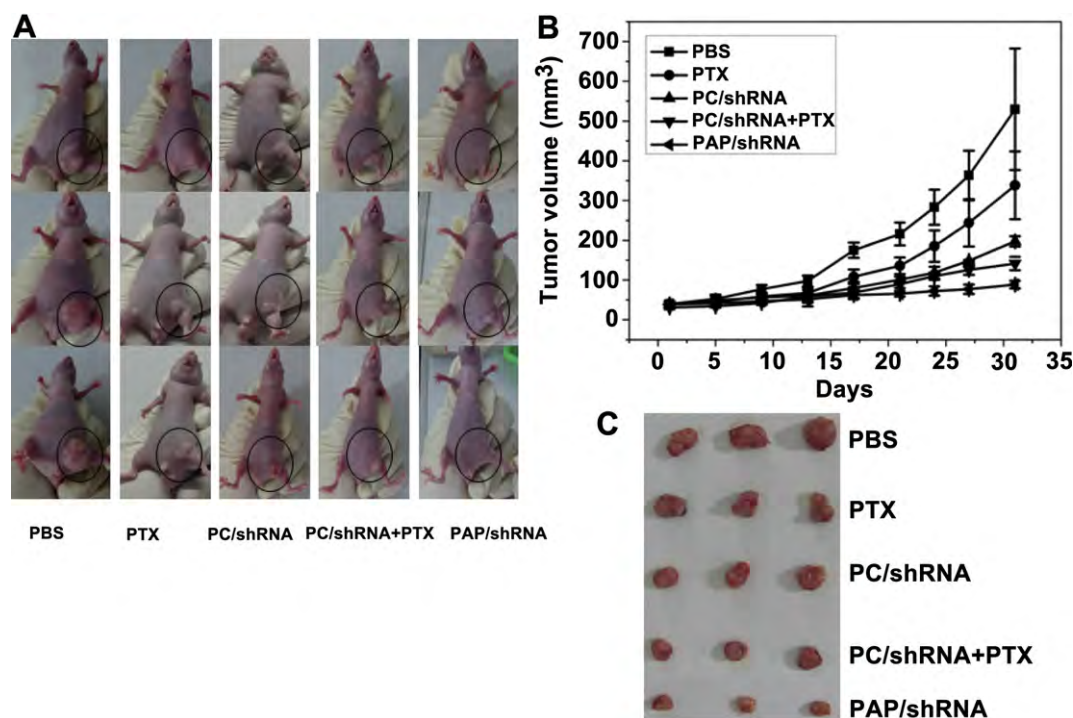


Fig. 8. Antitumoral therapeutic effects of PBS, PTX, PC/shRNA, PC/shRNA + PTX and PAP/shRNA complexes in tumor-bearing BALB/c: photo-images of *in vivo* tumor growth (A) and dissected tumor tissues (C) 30 days later after first treatment; (B) tumor volume changes with increasing time.

results indicate that the PTX and shRNA delivered simultaneously to the SKOV-3 cells by the supramolecular micelles enable efficient knockdown of survivin and Bcl-2 expression as well as synergistic cell apoptotic induction the *in vitro* study. Furthermore, the cytotoxicity of the PAP/shRNA and other various formations against SKOV-3 cells is evaluated to assess their anti-proliferative effects and the IC50 values are determined (Fig. 7 and Table 3). As expected, the PAP formulated to deliver survivin shRNA is the most cytotoxic at 48 h and 72 h, with the calculated IC50 values being: PAP/shRNA < PTX < PAP/SR < PAP < PC/shRNA < PC/SR.

3.4. *In vivo* antitumor activity

In the last set of experiments, we study whether the synergistic effects observed from PAP/shRNA *in vitro* can translate into tumor growth inhibition *in vivo*. Mice bearing SKOV-3 xenografts are treated with the PAP/shRNA and various other formulations by intra-tumoral injection from the 12th day after xenograft implantation twice a week for 2 weeks. The shRNA dose in each injection is 20 µg and the equivalent dose of PTX is 6 µg. As indicated in Fig. 8, five mice groups are tested including the normal saline (NS) control, free PTX, PC/shRNA, PAP/shRNA and PC/shRNA + PTX. Compared to other groups, the PAP/shRNA complexes are very effective in inhibiting tumor growth. The tumor growth is inhibited

sufficiently by the PAP/shRNA complexes at day 30. The tumor volume is less than 100 mm³ and much smaller than that observed from the other groups. The photographs and tumor weights of the dissected tumor tissues at day 30 are shown in Fig. 8B and C, respectively. The inhibition rate of the PAP/shRNA gene group is about 3.5 fold of that of the free PTX (Table 4).

4. Conclusion

Supramolecular micelles are prepared for simultaneous delivery of siRNA and a chemotherapeutic drug. This delivery system shows superiority in co-delivery of siRNA and PTX to the same tumor cells, synergistic knockdown of survivin and Bcl-2 expression, as well as cell apoptotic induction in the *in vitro* study. The supramolecular micelles simultaneously deliver survivin shRNA and PTX to yield good therapeutic effects in the inhibition of tumor growth. The results suggest that the combined delivery of survivin shRNA and PTX using the supramolecular micelles is an effective cancer therapy.

Acknowledgments

This work was jointly supported by the National High Technology Development Program of China (863 Program 2007AA03Z355), National Natural Science Foundation of China (Grant no. 30970711 and 21074111), National Basic Research Program (Grant no. 2010CB529902), Hong Kong Research Grants Council (RGC) General Research Funds (GRF) no. 112510, and City University of Hong Kong Applied Research Grant (ARG) no. 9667038.

References

- [1] Aagaard L, Rossi JJ. RNAi therapeutics: principles, prospects and challenges. *Adv Drug Deliv Rev* 2007;59:75–86.

- [2] Huang C, Li M, Chen C, Yao Q. Small interfering RNA therapy in cancer: mechanism, potential targets, and clinical applications. *Expert Opin Ther Targets* 2008;12:637–45.
- [3] Shapira A, Livney YD, Broxterman HJ, Assaraf YG. Nanomedicine for targeted cancer therapy: towards the overcoming of drug resistance. *Drug Resist Updat* 2011;14:150–63.
- [4] Ryan BM, O'Donovan N, Duffy MJ. Survivin: a new target for anti-cancer therapy. *Cancer Treat Rev* 2009;35:553–62.
- [5] Pennati M, Folini M, Zaffaroni N. Targeting survivin in cancer therapy. *Expert Opin Ther Targets* 2008;12:463–76.
- [6] Xu Z, Zhang Z, Chen Y, Chen L, Lin L, Li Y. The characteristics and performance of a multifunctional nanoassembly system for the co-delivery of docetaxel and iSur-pDNA in a mouse hepatocellular carcinoma model. *Biomaterials* 2010;31:916–22.
- [7] Xue HY, Wong HL. Tailoring nanostructured solid-lipid carriers for time-controlled intracellular siRNA kinetics to sustain RNAi-mediated chemosensitization. *Biomaterials* 2011;32:2662–72.
- [8] Wani MC, Taylor HL, Wall ME, Coggon P, McPhail AT. Plant antitumor agents. VI. The isolation and structure of taxol, a novel antileukemic and antitumor agent from *Taxus brevifolia*. *J Am Chem Soc* 1971;93:2325–7.
- [9] Schiff PB, Horwitz SB. Taxol stabilizes microtubules in mouse fibroblast cells. *Proc Natl Acad Sci USA* 1980;77:1561–5.
- [10] Singla AK, Garg A, Aggarwal D. Paclitaxel and its formulations. *Int J Pharm* 2002;235:179–92.
- [11] Luo C, Wang Y, Chen Q, Han X, Liu X, Sun J, et al. Advances of paclitaxel formulations based on nanosystem delivery technology. *Mini Rev Med Chem* 2012;12:434–44.
- [12] Heo DN, Yang DH, Moon HJ, Lee JB, Bae MS, Lee SC, et al. Gold nanoparticles surface-functionalized with paclitaxel drug and biotin receptor as theranostic agents for cancer therapy. *Biomaterials* 2012;33:856–66.
- [13] Zhang XQ, Xu X, Lam R, Giljohann D, Ho D, Mirkin CA. Strategy for increasing drug solubility and efficacy through covalent attachment to polyvalent DNA-nanoparticle conjugates. *ACS Nano* 2011;5:6962–70.
- [14] Yao HJ, Ju RJ, Wang XX, Zhang Y, Li RJ, Yu Y, et al. The antitumor efficacy of functional paclitaxel nanomicelles in treating resistant breast cancers by oral delivery. *Biomaterials* 2011;32:3285–302.
- [15] Wang X, Li J, Wang Y, Koenig L, Gjyzezi A, Giannakakou P, et al. A folate receptor-targeting nanoparticle minimizes drug resistance in a human cancer model. *ACS Nano* 2011;5:6184–94.
- [16] Chen Y, Bathula SR, Li J, Huang L. Multifunctional nanoparticles delivering small interfering RNA and doxorubicin overcome drug resistance in cancer. *J Biol Chem* 2010;285:22639–50.
- [17] Chen AM, Zhang M, Wei D, Stueber D, Taratula O, Minko T, et al. Co-delivery of doxorubicin and Bcl-2 siRNA by mesoporous silica nanoparticles enhances the efficacy of chemotherapy in multidrug-resistant cancer cells. *Small* 2009;5:2673–7.
- [18] Sun TM, Du JZ, Yao YD, Mao CQ, Dou S, Huang SY, et al. Simultaneous delivery of siRNA and paclitaxel via a “two-in-one” micelle promotes synergistic tumor suppression. *ACS Nano* 2011;5:1483–94.
- [19] Xiong XB, Lavasanifar A. Traceable multifunctional micellar nanocarriers for cancer-targeted co-delivery of MDR-1 siRNA and doxorubicin. *ACS Nano* 2011;5:5202–13.
- [20] Huang HY, Kuo WT, Chou MJ, Huang YY. Co-delivery of anti-vascular endothelial growth factor siRNA and doxorubicin by multifunctional polymeric micelle for tumor growth suppression. *J Biomed Mater Res A* 2011;97:330–8.
- [21] Hu QD, Fan H, Ping Y, Liang WQ, Tang GP, Li J. Cationic supramolecular nanoparticles for co-delivery of gene and anticancer drug. *Chem Commun (Camb)* 2011;47:5572–4.
- [22] Fan H, Hu QD, Xu FJ, Liang WQ, Tang GP, Yang WT. In vivo treatment of tumors using host-guest conjugated nanoparticles functionalized with doxorubicin and therapeutic gene pTRAIL. *Biomaterials* 2012;33:1428–36.
- [23] Chen G, Jiang M. Cyclodextrin-based inclusion complexation bridging supramolecular chemistry and macromolecular self-assembly. *Chem Soc Rev* 2011;40:2254–66.
- [24] Tang GP, Guo HY, Alexis F, Wang X, Zeng S, Lim TM, et al. Low molecular weight polyethylenimines linked by beta-cyclodextrin for gene transfer into the nervous system. *J Gene Med* 2006;8:736–44.
- [25] Lin C, Engbersen JF. Effect of chemical functionalities in poly(amido amine)s for non-viral gene transfection. *J Control Release* 2008;132:267–72.
- [26] Brummelkamp TR, Bernards R, Agami R. A system for stable expression of short interfering RNAs in mammalian cells. *Science* 2002;296:550–3.
- [27] Kim E, Jung Y, Choi H, Yang J, Suh JS, Huh YM, et al. Prostate cancer cell death produced by the co-delivery of Bcl-xL shRNA and doxorubicin using an aptamer-conjugated polyplex. *Biomaterials* 2010;31:4592–9.
- [28] Ikeguchi M, Ueda T, Sakatani T, Hirooka Y, Kaibara N. Expression of survivin messenger RNA correlates with poor prognosis in patients with hepatocellular carcinoma. *Diagn Mol Pathol* 2002;11:33–40.
- [29] Rosa J, Canovas P, Islam A, Altieri DC, Doxsey SJ. Survivin modulates microtubule dynamics and nucleation throughout the cell cycle. *Mol Biol Cell* 2006;17:1483–93.
- [30] Chen XQ, Yang S, Li ZY, Lu HS, Kang MQ, Lin TY. Effects and mechanism of downregulation of survivin expression by RNA interference on proliferation and apoptosis of lung cancer cells. *Mol Med Rep* 2012;5:917–22.